STRUCTURA, PROPRIETĂȚILE TERMOLUMINESCENTE ȘI PARAMETRII CINETICI AI SISTEMULUI VITROCERAMIC BOROSILICAT DOPAT CU GADOLINIU

STRUCTURE, THERMOLUMINESCENCE CHARACTERISTICS AND KINETIC PARAMETERS OF GADOLINIUM DOPED BOROSILICATE VITROCERAMIC SYSTEM

ANDRADA PASCU[1,2]*, ALIDA TIMAR-GABOR[2,3], AHMED KADARI[4,5], VIORICA SIMON[1,2]

[1]*Faculty of Physics, Babeş-Bolyai University, 1 Mihail Kogălniceanu, 400084 Cluj-Napoca, Romania*
[2]*Interdisciplinary Research Institute on Bio-Nano-Science of Babeş-Bolyai University, 42 Treboniu Laurean, 400271 Cluj-Napoca, Romania*
[3]*Faculty of Environmental Science and Engineering, Babeş-Bolyai University, 30 Fântânele, 400294 Cluj-Napoca*
[4]*Department of Chemistry, Faculty of Sciences of the Matter, IbnKhaldoun University of Tiaret, BP P 78 Zaaroura, Tiaret, Algeria*
[5]*Department of Physics, Electronic Microscopy and Materials Sciences Laboratory (EMMSL), B.P.1505 El M'Naouar, Oran, Algeria*

Structural characteristics of undoped and gadolinium doped melt-derived samples of SiO_2-B_2O_3 oxide system, as well as thermoluminescence (TL) properties and kinetic parameters of the sample with $40SiO_2{\cdot}59.5B_2O_3{\cdot}0.5Gd_2O_3$ composition were investigated in the present study. The gadolinium doped sample showed bright TL signal following irradiation with 6 Gy, good repeatability (under 10% deviation from the unit), linear dose dependence for the tested dose range (0.75 Gy – 9 Gy) and a minimum detectable dose of 34 mGy for instantaneous measurements. The kinetic parameters associated with the glow curves of $40SiO_2{\cdot}59.5B_2O_3{\cdot}0.5Gd_2O_3$ sample followed second order kinetics, while the value of the average activation energy was 0.88 eV. Both undoped and gadolinium doped samples were characterized by similar structural features.

În acest studiu au fost investigate caracteristicile structurale ale unor probe obținute prin metoda subrăcirii topiturilor în sistemul SiO_2-B_2O_3 atât nedopat, cât și dopat cu gadoliniu, precum și proprietățile termoluminescente (TL) și parametrii cinetici ai probei cu compoziția $40SiO_2{\cdot}59.5B_2O_3{\cdot}0.5Gd_2O_3$. În urma iradierii cu 6 Gy, proba dopată cu gadoliniu a fost caracterizată de un semnal TL luminos, repetabilitate bună (deviația de la unitate sub 10%), depedență liniară între doză și răspuns pentru intervalul de doze investigat (0,75 Gy – 9 Gy) și o doză minimă detectabilă de 34 mGy pentru măsurători imediate. Parametri cinetici asociați curbelor de strălucire a probei $40SiO_2{\cdot}59.5B_2O_3{\cdot}0.5Gd_2O_3$ au respectat cinetica de ordin 2, iar valoarea medie a energiei de activare a fost de 0,88 eV. Atât proba nedopată, cât și cea dopată au prezentat proprietăți structurale similare.

Keywords: *TGA, XRD, FTIR, thermoluminescence (TL), kinetic parameters, borosilicates*

1. Introduction

Accurate determination of radiation doses employed in various fields, such as nuclear installations, radiotherapy, environmental radiation physics and personal monitoring of ionizing radiation is an important and complex process, which continuously needs improving. Thus, new materials are now being developed in order to achieve high precision dosimeters characterized by thermo-luminescence (TL) sensitivity and linearity over a broad range of doses. The dosimetric properties of luminescent materials are related to the kinetic parameters which quantitatively describe the trap and recombination centers involved in the thermoluminescent emission of light and they can be determined using different techniques such as initial rise method, heating rate methods, isothermal decay analysis methods or Chen`s peak shape method [1].

Rare-earth doped luminescent materials play a significant part as radiation detectors due to the fact that incorporating rare-earths as dopants into the host may improve the stability and/or enhance the sensitivity of the dosimeter [2, 3]. Numerous studies have explored the suitability of silicates, alkali silicates, alkali aluminosilicates and borosilicates doped with rare-earth ions and transition metal ions in radiation dosimetry applications [2, 4-10]. Compared to other amorphous materials, borosilicate glasses exhibit superior properties in terms of thermal stability, chemical durability, mechanical resistance, cost and availability, while doped with especially high concentration of Gd_2O_3 borosilicates are attractive materials in luminescent field [11]. Borosilicate glasses are characterized by four types of traps: network microstructure defect (E'-defect), non-bridging oxygen hole centers, multivalent ion centers, and network modifier defects [7].

* Autor corespondent/*Corresponding author*,
E-mail: adarox_pascu@yahoo.com

The dissolution mechanism of gadolinium in borosilicate glasses revealed that gadolinium first partitions to the borate-rich environment in the form of Gd-metalborate-like structure at low Gd_2O_3 concentrations and then to the silicate-rich environments causing the breaking of Si-O-Si bonds and the forming of non-bridging oxygen at high Gd_2O_3 concentrations [12].

In the present study, the thermoluminescence characteristics of 40SiO2·59.5B2O3·0.5Gd2O3 vitroceramic system were investigated in terms of TL intensity, repeatability, dose dependence, and minimum detectable dose along with its kinetic parameters using the Chen`s peak shape method. The compound was also structurally characterized by thermal analysis (TGA/DTA), X-ray diffraction (XRD) and infrared spectroscopy (FT-IR) both before and after adding Gd^{3+} ions in the host material.

2. Materials and methods

2.1. Vitroceramic preparation

The investigated vitroceramic sample, with $40SiO_2 \cdot 59.5B_2O_3 \cdot 0.5Gd_2O_3$ mol% nominal composition, was prepared by melting mechanically homogenized mixtures of H_3BO_3, SiO_2 and Gd_2O_3 analytical reagents of p.a. purity at 1400°C for 15 minutes followed by fast undercooling to room temperature. The value chosen for the ratio between SiO_2 and B_2O_3 aimed to reduce the phase separation tendency governing the binary SiO_2-B_2O_3 glass system in the silica rich composition range [13, 14].

2.2. Thermal and structural characterization techniques

Thermal analysis (DTA and TGA) was conducted on a Shimadzu derivatograph DTG-60H at a heating rate of 10°C/min, from room temperature up to 1100°C. Alumina open crucibles and α-alumina powder as reference material were used, and the measurements were performed in a dynamic nitrogen and air atmosphere at a flow rate of 70 ml/min.

The X-ray diffraction (XRD) investigations were conducted with a Shimadzu XRD-6000 diffractometer, using Cu-K_α radiation (λ = 1.5418 Å), with Ni–filter. The XRD patterns were recorded in the 2θ scan range 10-80°, with a scan speed of 2°/min, using quartz powder as calibrating material. The operating power of the X-ray source was 40 kV at 30 mA intensity.

Fourier transform infrared (FTIR) spectra were recorded in reflection configuration in the range 4000-400 cm^{-1} with a resolution of 4 cm^{-1} using a Jasco FT-IR-6200 Spectrometer and KBr pellet technique.

2.3. Thermoluminescence measurements

All measurements were performed with a Risø TL/OSL Luminescence Reader model TL/OSL-DA-20. Irradiations were performed using the built-in ^{90}Sr-^{90}Y beta source delivering 0.145 Gy/s (absorbed dose rate in quartz). TL signals were registered up to 500°C, using a controlled heating rate of 5°C/s and no initial thermal treatments were applied. The luminescence emissions were measured using a bialkali EMI 9235QA photomultiplier tube through a Hoya U-340 filter (270-370 nm). The vitroceramic sample was measured in the form of powder and after investigations each aliquot was weighed for mass normalization.

3. Results and discussion

3.1. Thermal analysis (TGA/DTA)

Figure 1 shows the differential thermal (DTA) and thermogravimetric (TGA) curves obtained for the undoped and gadolinium doped borosilicate sample.

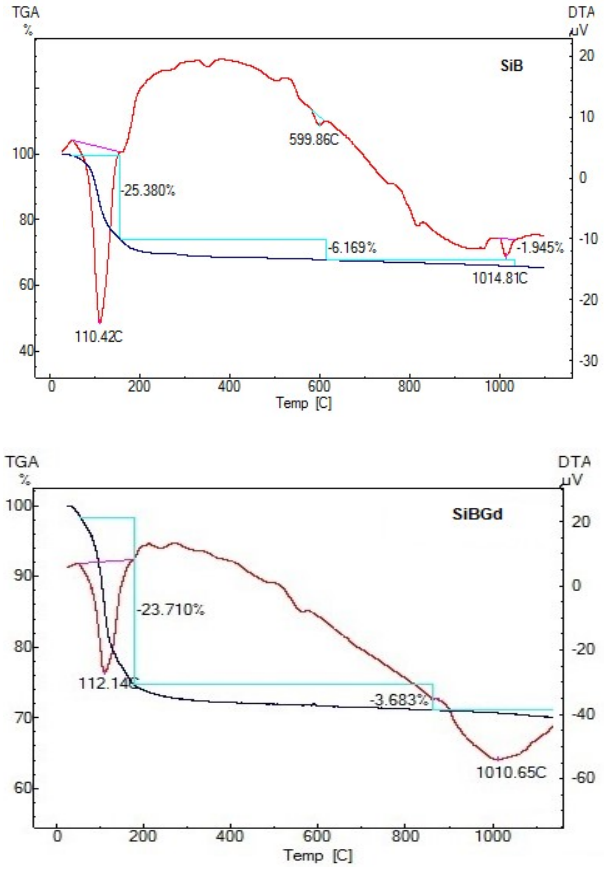

Fig. 1 - TGA and DTA curves of the undoped and gadolinium doped borosilicate vitroceramic system. *Curbele TGA și DTA ale sistemului vitroceramic borosilicat nedopat și dopat cu gadoliniu.*

The DTA and TGA analyses point out that in DTA runs a major endothermic event, close to 110°C, accompanied by mass loss due to removal of physically adsorbed water. By further heating, a mass loss assigned to dihydroxylation is recorded.

The weak thermal events observed in DTA traces up to 1000°C could evidence slight rearrangements in the local structure of the samples. The endothermic event recorded around 1010°C denotes softening and the beginning of melting process. The thermal behavior of the undoped and gadolinium doped samples is very similar, except the endothermic event at 1010°C, which in the case of gadolinium doped borosilicate system has a larger extent. This disparity denotes the gadolinium contribution in breaking the bonds of the borosilicate matrix.

3.2. X-ray diffraction (XRD)

A high similarity of the diffractions patterns of undoped and gadolinium doped borosilicate sample both before and after irradiation is observed (see Fig. 2). The diffraction peaks occurring at 2Θ angles 14.6, 27.8, 30.6 and 40.0° are typical for B_2O_3 crystalline phase (ICCD PDF # 06-0297). The aforementioned crystalline phase can be developed during sample cooling due to a weak, partial crystallization easily achievable in the binary borosilicate melts wherein glass-in-glass phase separation is very likely [15, 16].

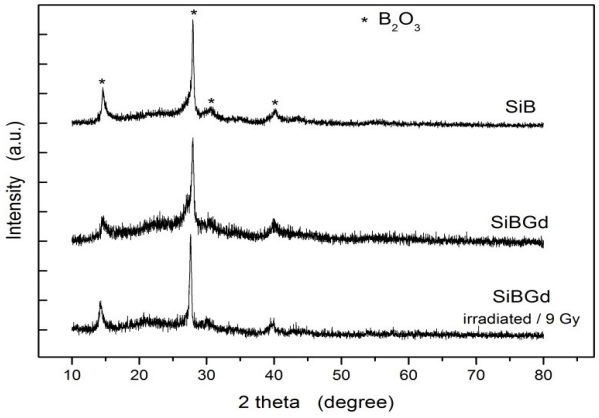

Fig. 2 - X-ray diffractograms of the undoped borosilicate and gadolinium doped borosilicate both before and after beta irradiation with 9 Gy. *Difractogramele de raze X ale borosilicatului nedopat și dopat cu gadoliniu, atât înainte, cât și după iradierea cu 9 Gy folosind sursa beta.*

Nevertheless, it can be seen that the Gd_2O_3 addition leads to an increased disorder degree, as denoted by the large bump in 2Θ range 20-35°, and to smaller crystallites size, as denoted by the wider diffraction lines. The crystallite size determined with Scherrer equation, based on line width at half maximum intensity, is 46.6 nm for the undoped sample and 20.4 nm for the gadolinium doped sample. This result is due to Gd_2O_3 ability to promote the silicate network polymerization. Also, weakly higher crystallite size of 27.9 nm is observed for the gadolinium doped sample after irradiation related to the improvement of B_2O_3 crystallinity. Usually the high dose radiation induces an increase in silicate network polymerization [17]. Increase of crystallinity after low dose irradiation was reported for polymers, and explained by shorting of polymer chain and increasing in mobility that favors the crystallites growth in the amorphous regions [18]. An increase of crystallinity after irradiation was reported also for amorphous alloy thin films γ-irradiated with 25-100 kGy doses [19].

3.3. Infrared spectroscopy (FTIR)

The infrared spectra of undoped and Gd doped borosilicate are depicted in Figure 3. The absorption band at 3221 cm^{-1} is assigned to vibrations of molecular water, which may also contribute to the 1650 cm^{-1} shoulder, while the bands around 2513, 2364 and 2262 cm^{-1} are assigned to vibrations of silicon bonds, carbon dioxide contamination, and Si-O-Si stretching vibrations, respectively [20, 21]. The dominant band at 1465 cm^{-1} and the shoulder at 1383 cm^{-1} are attributed to bending and stretching vibrations of B–O–B in (BO_3) units, while the band at 1060 cm^{-1} to Si-O-Si stretching. The band at 787 cm^{-1} is attributed both to Si-O-Si stretching and B-O-B bending vibrations in (BO_4) units, the shoulder at 736 cm^{-1} to B-O-B bending in (BO_3) units, 644 cm^{-1} to O-B-O and Si-O-B, 541 cm^{-1} to Si-O-B, and 449 cm^{-1} to Si-O-Si, O-Si-O and B-O-B bending vibrations [17, 22-24]. The narrow infrared band at 885 cm^{-1} could be assigned to vibrations of tricoordinated boron atoms partly bound to the network, and to which a hydroxyl group is attached [25, 26]. In agreement with XRD results, the FTIR analysis indicates that the small amount of Gd_2O_3 added to the borosilicate matrix sensibly affects the 1060 cm^{-1} band which may be related to silica vitreous phase. After irradiation the intensity of 1060 cm^{-1} band is diminished due to the slight increase in sample crystallinity.

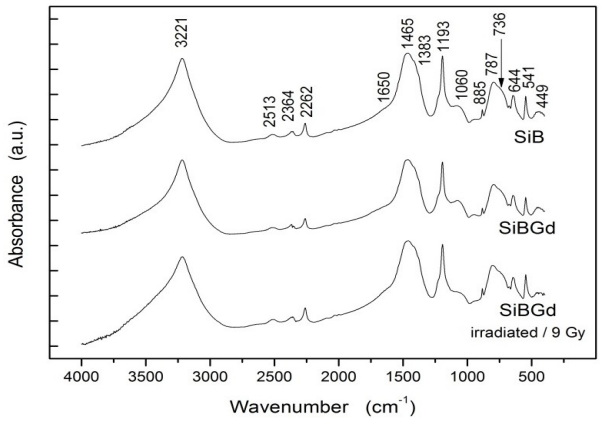

Fig. 3 - FTIR spectra of the undoped borosilicate and gadolinium doped borosilicate both before and after beta irradiation with 9 Gy. *Spectrele FTIR ale borosilicatului nedopat și dopat cu gadoliniu, atât înainte, cât și după iradierea cu 9 Gy folosind sursa beta.*

3.4. Thermoluminescence glow curves and repeatability

TL glow curves of three aliquots consisting of $40SiO_2 \cdot 59.5B_2O_3 \cdot 0.5Gd_2O_3$ mol% were recorded after beta irradiation with 6 Gy using a controlled heating rate (5°C/s) and without applying prior preheat treatments. Following irradiation, the aliquots showed similar glow curves in terms of TL signal intensity, position and shape of the glow peak. The obtained TL glow curves are depicted in Figure 4.

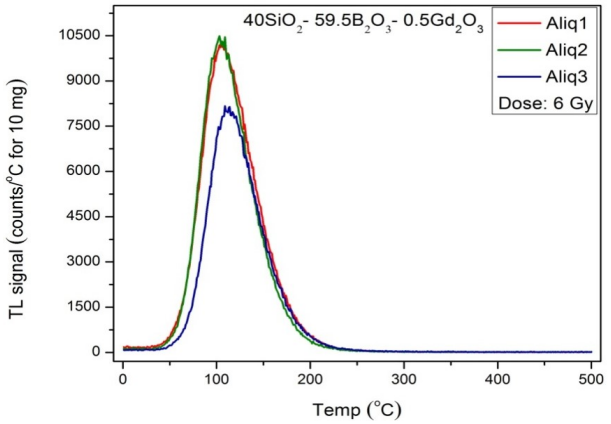

Fig. 4 - TL glow curves of three aliquots consisting of $40SiO_2 \cdot 59.5B_2O_3 \cdot 0.5Gd_2O_3$ mol% measured after irradiation with 6 Gy. TL glow curves are normalized to a mass of 10 mg of sample. *Curbele de strălucire a trei alicote constând în $40SiO_2 \cdot 59.5B_2O_3 \cdot 0.5Gd_2O_3$ %mol măsurate după iradierea cu 6 Gy. Curbele de strălucire sunt normalizate la o masă de 10 mg de probă.*

Therefore, the glow curves of the samples were composed by two overlapping peaks, with the maximum TL intensity of the dominant peak ranging between approximately 8,000 and 10,500 counts for 10 mg of sample, while the peaks position was placed around 100-110°C. The repeatability of the TL signals was also investigated. As such, two aliquots of the vitroceramic system were subjected to five irradiation-readout cycles using a constant dose of 6 Gy and the signals were instantly measured after irradiation. The signal obtained in each measurement cycle was then normalized to the initial response, corresponding to the first irradiation-readout cycle. Both aliquots where characterized by a slight sensitization, with less than 10% deviation from the first readout.

3.5. Thermoluminescence growth curves and MDD

The TL dose dependence of $40SiO_2 \cdot 59.5B_2O_3 \cdot 0.5Gd_2O_3$ vitroceramic system was investigated using the single aliquot regeneration protocol, which was applied on three aliquots. After measuring the native signal of the samples, their growth curves were raised by irradiating the aliquots with five increasing doses (0.75, 1.5, 3, 6, 9 Gy) and subsequently measuring the TL response by ramp heating to 500°C.

The selected region of interest for integrating TL signals was 60-300°C. The obtained results indicated a linear dose response of the samples in the investigated dose range (see Fig. 5), with an average sensitivity or specific luminescence, which is given by the slope of the growth curves, of ~106,000 counts for a mass of 10 mg.

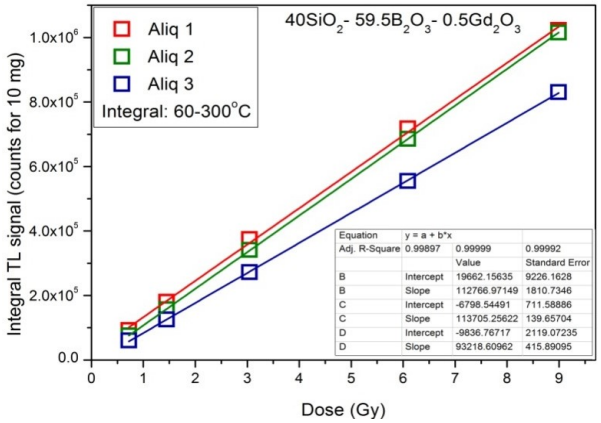

Fig. 5 - TL dose response growth curves of three aliquots consisting of $40SiO_2 \cdot 59.5B_2O_3 \cdot 0.5Gd_2O_3$ mol% for the selected region of interest (60-300°C). Mass normalization has been carried out for each aliquot. *Curbele TL de creștere a semnalului în funcție de doză a trei alicote constând în $40SiO_2 \cdot 59.5B_2O_3 \cdot 0.5Gd_2O_3$ %mol pentru intervalul de interes (60-300°C). Normalizarea la masă a fost efectuată pentru fiecare alicotă.*

The minimum detectable dose (MDD) was estimated as the dose for which the signal is three times the standard deviation of the native signal. The Gd doped borosilicate was characterized by a MDD value of 34 mGy for instantaneous measurements.

3.6. Kinetic parameters

The kinetic parameters (order of kinetics (b), activation energy (E), frequency factor (s)) of the $40SiO_2 \cdot 59.5B_2O_3 \cdot 0.5Gd_2O_3$ vitroceramic system were determined using Chen`s method [27]. This technique is based on the general geometry of the generated peak in the TL glow curve, considering the total half intensity width ($\omega = T_2 - T_1$), the high-temperature half width ($\delta = T_2 - T_m$) and the low-temperature half width ($\tau = T_m - T_1$), where T_m is the peak temperature at the maximum TL intensity, T_1 (rising end) and T_2 (falling end) are the temperatures on either side of T_m, corresponding to the half intensity of the glow peak.

Chen's method does not require knowledge of the kinetic order, which is determined by using the geometry factor (μ_g) from the peak shape. When $\mu_g \approx 0.42$, the recombination process follows first order kinetics, while the kinetics are second order when $\mu_g \approx 0.52$. The following equation is used for determining the order of kinetics:

Table 1

Kinetic parameters of the deconvoluted peaks obtained for $40SiO_2 \cdot 59.5B_2O_3 \cdot 0.5Gd_2O_3$ vitroceramic system determined by applying Chen`s peak shape method. *Parametri cinetici ai sistemului vitroceramic $40SiO_2 \cdot 59.5B_2O_3 \cdot 0.5Gd_2O_3$ obținuți prin aplicarea metodei lui Chen după deconvoluția componentelor din curbele de strălucire ale alicotelor.*

	T_m (K)	μ_g	b	E_ω (eV)	E_τ (eV)	E_δ (eV)	$E_{average}$ (eV)	s (s^{-1})
Aliq 1	372	0.52	2.00	0.848	0.821	0.864	0.844	8.95×10^{10}
	414	0.52	2.00	0.899	0.899	0.893	0.897	2.33×10^{10}
Aliq 2	371	0.52	2.00	0.859	0.860	0.852	0.857	1.47×10^{11}
	409	0.52	2.00	0.894	0.893	0.888	0.891	2.73×10^{10}
Aliq 3	378	0.52	2.00	0.881	0.897	0.862	0.879	1.74×10^{11}
	416	0.52	2.00	0.960	0.965	0.949	0.958	1.20×10^{11}

$$\mu_g = \frac{T_2 - T_m}{T_2 - T_1} \quad (1)$$

Based on the value of the kinetic order, the activation energy is determined using the following equation:

$$E_\alpha = c_\alpha \left(\frac{kT_m^2}{\alpha}\right) - b_\alpha (2kT_m) \quad (2)$$

where α corresponds to τ, δ and ω, respectively, and k is the Boltzmann constant ($k = 8.6\times10^{-5}$ eV.K^{-1}). The expressions for c_α and b_α are summarized below:

$$c_\tau = 1.51 + 3(\mu_g - 0.42), \quad b_\tau = 1.58 + 4.2(\mu_g - 0.42) \quad (2.1)$$

$$c_\delta = 0.976 + 7.3(\mu_g - 0.42), \quad b_\delta = 0 \quad (2.2)$$

$$c_\omega = 2.52 + 10.2(\mu_g - 0.42), \quad b_\delta = 1 \quad (2.3)$$

The frequency factor is given by the following relationship:

$$s = \frac{\beta E}{kT_m^2} exp\left(\frac{E}{kT_m^2}\right)\left[1 + (b-1)\frac{2kT_m}{E}\right]^{-1} \quad (3)$$

where β is the linear heating rate (β = 5°C.s^{-1}).

After the glow curve deconvolution of the investigated Gd doped borosilicate aliquots, the kinetic parameters were determined for each composing peak of the glow curves depicted in Fig 4. The results are presented in Table 1.

4. Conclusions

In this work, the structural characteristics, thermoluminescence properties and kinetic parameters of $40SiO_2 \cdot 59.5B_2O_3 \cdot 0.5Gd_2O_3$ vitroceramic system containing B_2O_3 nanocrystallites were analyzed. A slight crystallites growth was observed after beta irradiation with 9 Gy. The TL glow curves of beta irradiated samples were composed by two overlapping peaks, with the maximum TL intensity of the dominant peak ranging between approximately 8,000 and 10,500 counts for 10 mg of sample, while the peaks position was placed around 100-110°C. Moreover, a good repeatability and high linearity for the investigated dose range (0.75-9 Gy) were observed, whereas the minimum detectable dose for instantaneous measurements was 34 mGy. After glow curve deconvolution, the kinetic parameters of the composing peaks were determined using Chen`s peak shape method. All gadolinium doped borosilicate glow curves followed second order kinetics and their activation energy average values varied between 0.844 and 0.958 eV.

REFERENCES

1. A. Kadari, A. Pascu, A. Timar-Gabor, V. Simon, D. Kadri, Trapping parameters determination and modeling of the thermoluminescence process in SiO_2-P_2O_5 vitroceramics doped with different Y_2O_3 concentrations, Optik, 2016, **127**, 6162.
2. R. Laopaiboon, C. Bootjomchai, Thermoluminescence studies on alkali-silicate glass doped with dysprosium oxide for use in radiation dosimetry measurement, Journal of Luminescence, 2015, **158**, 275.
3. Y.S.M. Alajerami, S. Hashim, S.K. Ghoshal, M.A. Saleh, T. Kadni, M.I. Saripan, K. Alzimami, Z. Ibrahim, D.A. Bradley, The effect of TiO_2 and MgO on the thermoluminescence properties of a lithium potassium borate glass system, Journal of Physics and Chemistry of Solids, 2013, **74**, 1816.
4. B. Biró, A. Pascu, A. Timar-Gabor, V. Simon, Thermoluminescence investigations on $xY_2O_{31}\cdot(60-x)P_2O_5\cdot40SiO_2$ vitroceramics, Applied Radiation and Isotopes, 2015, **98**, 49.
5. R.A. Barve, N. Suriyamurthy, B.S. Panigrahi, B. Venkatraman, Dosimetric investigations of Tb^{3+}-doped strontium silicate phosphor, Radiation Protection Dosimetry, 2014, **163**, 430.
6. R.R. Patil, R. Barve, S.V. Moharil, M.S. Kulkarni, B.C. Bhatt, Development of Ag doped crystalline SiO_2 for possible applications in real-time in-vivo OSL dosimetry, Radiation Measurements, 2014, **71**, 208.
7. R.A. Clark, J.D. Robertson, J.M. Schwantes, Intrinsic dosimetry: elemental composition effects on the thermoluminescence of commercial borosilicate glass, Radiation Measurements, 2013, **59**, 170.
8. M. Prokić, E.G. Yukihara, Dosimetric characteristics of high sensitive Mg_2SiO_4:Tb solid TL detector, Radiation Measurements, 2008**,** **43**, 463.
9. J.C. Mittani, M. Prokić, E.G. Yukihara, Optically stimulated luminescence and thermoluminescence of terbium-activated silicates and aluminates, Radiation Measurements, 2008, **43**, 323.
10. A.L. Yusoff, R.P. Hugtenburg, D.A. Bradley, Review of development of a silica-based thermoluminescence dosimeter, Radiation Physics and Chemistry, 2005, **74**, 459.
11. H. Luo, X. Hu, W. Liu, Y. Zhang, A. Lu, X. Hao, Compositional dependence of properties of Gd_2O_3-SiO_2-B_2O_3 glasses with high Gd_2O_3 concentration, Journal of Non-Crystalline Solids, 2014, **389**, 86.

12. H. Li, Y. Su, L. Li, D.M. Strachan, Raman spectroscopic study of gadolinium (III) in sodium-aluminoborosilicate glasses, Journal of Non-Crystalline Solids, 2001, **292**, 167.
13. I.G. Polyakova, Alkali borosilicate systems: Phase diagrams and properties of glasses, Physics and Chemistry of Glasses, 2000, **41**, 247.
14. M.J. Plodinec, Borosilicate glasses for nuclear waste imobilisation, Glass Technology, 2000, **41**, 186.
15. R.J. Charles, F.E. Wagstaff, Metastable immiscibility in the B_2O_3–SiO_2 system, Journal of the American Ceramic Society, 1968, **51**, 16.
16. O.V. Mazurin, G.P. Roskova, E.A. Porai-Koshits, Immiscibility diagrams of oxide glass-forming systems, In Phase Separation in Glass, Edited by O.V. Mazurin, and E.A. Porai-Koshits. Elsevier Science Publishers, B. V., Amsterdam, 1984, 103.
17. O.J. McGann, P.A. Bingham, R.J. Hand, A.S. Gandy, M. Kavcic, M. Zitnik, K. Bucar, R. Edge, N.C. Hyatt, The effects of γ-radiation on model vitreous wasteforms intended for the disposal of intermediate and high level radioactive wastes in the United Kingdom, Journal of Nuclear Materials, 2012, **429**, 353.
18. Z. Zhudi, Y. Wenxue, C. Xinfang, Study on increase in crystallinity in γ-irradiated poly (vinylidene fluoride), Radiation Physics and Chemistry, 2012, **65**, 173.
19. S. Ahmad, K. Asokan, M. Zulfequar, Effect of Gamma Irradiation on Structural and optical properties of Thin Films of a-$Cd_5Se_{95-x}Zn_x$, International Journal of Thin Films Science and Technology, 2015, **4**, 103.
20. A. Deptula, M. Milkowska, W. Lada, T. Olczak, D. Wawszczak, T. Smolinski, F. Zaza, M. Brykala, A.G. Chmielewski, K.C. Goretta, Sol-gel processing of silica nuclear waste glasses, New Journal of Glass and Ceramics, 2011, **1**, 105.
21. T. Uchino, A. Aboshi, S. Kohara, Y. Ohishi, M. Sakashita, K. Aoki, Microscopic structure of nanometer-sized silica particles. Physical Review B, 2004, **69**, 155409-1.
22. C. Gautam, A.K. Yadav, A.K. Singh, A review on infrared spectroscopy of borate glasses with effects of different additives, ISRN Ceramics, 2012, doi:10.5402/2012/428497.
23. T.I. Avdeeva, I.A. Vorsina, IR spectra of low-silica sodium hydroaluminosilicates, Bulletin of the Academy of Sciences of the USSR Division of Chemical Science, 1969, **18**, 20151.
24. M.S. Gaafar, S.Y. Marzouk, Mechanical and structural studies on sodium borosilicate glasses doped with Er_2O_3 using ultrasonic velocity and FTIR spectroscopy, Physica *B*, 2007, **388**, 294.
25. L. Baia, R. Stefan, J. Popp, S. Simon, W. Kiefer, Vibrational spectroscopy of highly iron doped B_2O_3-Bi_2O_3 glass systems, Journal of Non-Crystalline Solids, 2003, **324**, 109.
26. A. Vimont, F. Thibault-Starzyk, J.C. Lavalley, Infrared spectroscopic study of the acidobasic properties of beta zeolite, Journal of Physical Chemistry B, 2000, **104**, 286.
27. R. Chen, On the calculation of activation energies and frequency factors from glow curves, Journal of Applied Physics, 1969, **40**, 570.

****

MANIFESTĂRI ȘTIINȚIFICE / SCIENTIFIC EVENTS

5th Nano Today Conference

December 6-10, 2017 | Waikoloa Beach Marriott, Hawaii, USA

Organized by the *Nano Today* journal, the Institute of Bioengineering and Nanotechnology (IBN) and Elsevier, the 5th Nano Today Conference (Nano Today 2017) seeks to bring together researchers interested in nanoscience and nanotechnology.

Topics

- Synthesis and Self-Assembly of Nanocrystals, Nanoparticles and Thin Films
- Functionalization and Size-Dependent Properties of Nanocrystals, Quantum Dots and Nanowires
- Processing and Templating of Nanotubes and Nanoporous Materials
- Tailoring of Polymeric Nanoparticles, Organic-Inorganic Nanocomposites and Biohybrids
- Nanosystems for Biological and Medical Applications
- Nanosystems for Sensing, Diagnostic, Imaging, Magnetic, Electronic and Structural Applications
- Nanomaterials for Energy and Environmental Applications
- Nanomaterials for Chemical and Catalytic Applications

****